Thin Film Nanocomposite Forward Osmosis Membranes

Forward osmosis (FO) is a low-energy treatment process driven by osmosis to induce the separation of water from dissolved solutes/foulants through the membrane in hydraulic pressure absence while retaining all of these materials on the other side.

1. Introduction

In past decades, freshwater demand has risen substantially owing to population growth, economic development, and different consumption patterns [1]. This ultimately, induced a global clean water scarcity and this scenario will only get worse in the next few decades. According to the United Nations, the lack of safe drinking water will affect nearly 6 billion people by 2050. **Figure 1** provides details on global water supply, freshwater supply, and freshwater use according to UN-Water. As a consequence, to address the impending global freshwater shortage problem, sustainable, cost-effective desalination technologies are a necessity to exploit the infinite salty water resources available on the planet [2].
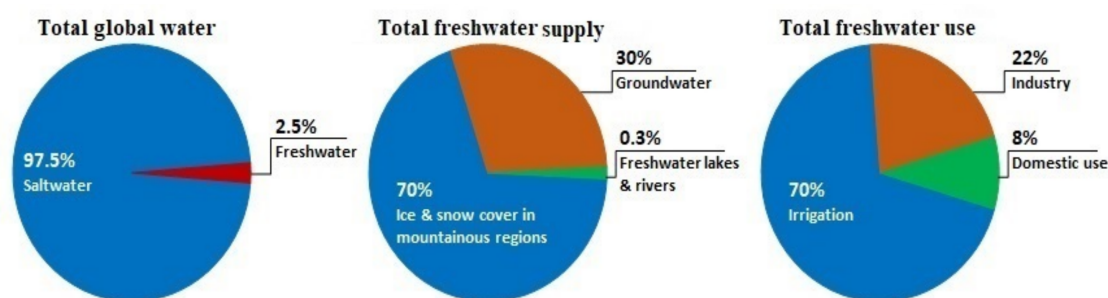

Figure 1. Information about global water and global supply and use of freshwater according to UN-Water "everythingconnects.org/fresh-water (accessed on 25 December 2022)".

One of these reliable desalination technologies is membrane-based technologies. Membrane technology is gaining increasing popularity in water, wastewater, and many other industrial applications and is divided into (I) pressure-driven membrane processes (PDMPs) such as microfiltration (MF), ultrafiltration (UF), nanofiltration (NF), and reverse osmosis (RO) [3][4][5][6] and (II) osmotically-driven membrane processes (ODMPs) such as forward osmosis (FO) and pressure retarded osmosis (PRO) [6][7]. PDMPs, especially RO, have attracted much attention in water treatment processes due to their high productivity for pure water. Nevertheless, most of these membrane processes are energy-consuming and high-priced [8]. This drawback has led to the investigation of alternate means of desalinating water. ODMPs, especially FO, as an alternative to PDMPs have seen immense attraction within membrane science in recent years [7]. FO as an emerging membrane technology has received tremendous attention recently for its use in water purification [9].

2. Thin Film Nanocomposite FO Membranes

With the considerable advancements in nanotechnology, the incorporation of nanoparticles into the substrate as well as into the active layer of TFC membranes is attractive because it enables changes in membrane performance without significantly altering the intrinsic membrane structure. In general, nanoparticles-modified TFC membranes in most investigations have demonstrated much higher water flux compared to unmodified TFC membranes due to increased membrane porosity, hydrophilicity, and decreased support layer tortuosity, which mitigates the ICP effect [10]. **Table 1**

summarizes numerous studies on nanoparticle-modified TFC membranes that have been published in the literature. The table comprises water flux and reverse salt flux with an active layer in the two different modes of AL-FS and AL-DS.

Table 1. Summary of the studies on FO performance of nanoparticle-modified TFC membranes.

Support Layer Polyamide Active Layer Nanomaterial	Experimental Operating Conditions				FO Performance				Intrinsic Properties	Reference
	Feed Solution	Draw Solution	Temp.	Flow Rate	FS–AL (FO Mode)		DS–AL (PRO Mode)			
					Jw; LMH	Js; gMH	Jw; LMH	Js; gMH		
14% PSF/1% PVP 2% MPD/0.1% TMC 0.04% MOF in organic solution	DI water	2M NaCl	25 °C	21 cm/s	46	102.3	—	—	A = 4.7 LMH/bar B = 0.6 LMH S = 238 μm	[11]
16% PSF 2% MPD/0.15% TMC 0.25% GO in dope solution	DI water	0.5M NaCl	25 °C	1.8 L/min	19.77	3.4	40.5	6.5	A = 1.76 LMH/bar B = 0.19 LMH R (NaCl) = 98.71% S = 191 μm	[12]
18% PSF 2% MPD/0.1% TMC 0.25% GO in dope solution	DI water	1M NaCl	24 °C	1.5 L/min	14.65	3.62	30.95	6.6	A = 1.91 LMH/bar B = 0.24 LMH R (NaCl) = 98.67% S = 726 μm	[13]
12% PSF 4% MPD/0.1% TMC 0.01% GO-8h in aqueous solution	DI water	0.5M NaCl	22 °C	12.6 cm/s	24.7	5.19	41.9	8	A = 3.71 LMH/bar B = 0.89 LMH	[14]
16% PSF/4% PEG-400 2% MPD/0.1% TMC 0.008% GO in aqueous solution	DI water	2M NaCl	—	12 L/h	34.3	1.1	—	—	B = 3.9 LMH/bar A = 1.1 LMH R (NaCl) = 96.7% S = 119 μm	[15]
15.5% PSF/0.5% PVP/3% LiCl 1% MPD/0.05% TMC 0.02% zeolite in organic solution	DI water	1M NaCl	—	0.5 L/min	13.8	7.08	28.8	13.76	A = 5.27 × 10^{-12} m/s.Pa B = 15.1 × 10^{-8} m/s R (NaCl) = 88.1%	[16]
15.5% PSF/0.5% PVP/3% LiCl 1% MPD/0.05% TMC 0.5% zeolite in dope solution	DI water	2M NaCl	—	0.5 L/min	40	29	86	57	A = 3.3 LMH/bar R (NaCl) = 91.3% S = 340 μm	[17]
15.5% PSF/2% PVP 2% MPD/0.1% TMC 0.4% zeolite in dope solution	10 mM NaCl	2M NaCl	room	0.8 L/min	24.61	14.6	33.1	20	A = 6.86 × 10^{-12} m/s.Pa B = 9.6 × 10^{-8} m/s R (NaCl) = 94.7% S = 480 μm	[18]
16.5% PSF/0.5% PVP 2% MPD/0.15% TMC 0.6% TiO_2 in dope solution	DI water	2M NaCl	ambient	0.35 L/min	33	15.7	59.4	31	A = 7.3 × 10^{-12} m/s.Pa B = 12.4 × 10^{-8} m/s R (NaCl) = 93.6% S = 390 μm	[19]

Support Layer Polyamide Active Layer Nanomaterial	Experimental Operating Conditions				FO Performance				Intrinsic Properties	Reference
	Feed Solution	Draw Solution	Temp.	Flow Rate	FS–AL (FO Mode)		DS–AL (PRO Mode)			
					Jw; LMH	Js; gMH	Jw; LMH	Js; gMH		
17.41% PSF/0.5% PVP 2% MPD/0.1% TMC 0.5% TiO_2 in dope solution	10 mM NaCl	2M NaCl	ambient	32.72 cm/s	29.7	7.3	56.27	14.14	A = 5.45 × 10^{-12} m/s.Pa B = 10.66 × 10^{-8} m/s R (NaCl) = 92.7% S = 420 µm	[20]
16% PSF 2% MPD/2% TEA/0.2% TMC 0.1% TiO_2 in aqueous solution	10 mM NaCl	2M NaCl	—	0.8 L/min	40	12.3	26	13	A = 12.26 × 10^{-12} m/s.Pa B = 49.9 × 10^{-8} m/s R (NaCl) = 86% S = 650 µm	[21]
16% PEF/1% PVP/2.5% PEG-200 2% MPD/0.1% TMC 0.05% SiO_2 in aqueous solution	DI water	2M NaCl	30 °C	10 L/h	15.22	7.53	23.93	16.15	A = 3.10 LMH/bar B = 0.31 LMH R (NaCl) = 91% S = 362 µm	[22]
16% PSF/1% PVP 2% MPD/0.1% TMC 0.05% SiO_2 in aqueous solution	10 mM NaCl	2M NaCl	30 °C	0.8 L/min	15	1.6	25.28	3.44	A = 9.52 × 10^{-12} m/s.Pa B = 28.4 × 10^{-8} m/s R (NaCl) = 89% S = 368 µm	[23]
14% PSF/0.5% PVP 1% MPD/0.05% TMC 1% SiO_2 in dope solution	DI water	2M NaCl	25 °C	0.25 L/min	14.60	9.00	23.50	20.06	A = 2.96 × 10^{-12} m/s.Pa B = 4.79 × 10^{-8} m/s R (NaCl) = 86.18%	[24]
E.Spun N6/20% SiO_2 1% MPD/0.15% TMC 4% SiO_2 in aqueous solution	DI water	1M NaCl	24 °C	26.3 cm/s	27.10	9.35	—	—	A = 45 LMH/MPa B = 1.24 LMH R (NaCl) = 98.5% S = 365 µm	[25]
14% PSF/ 2%PVP 2% MPD/0.1% TMC 0.5% ZnO in dope solution	10 mM NaCl	2M NaCl	—	—	30.06	17.31	—	—	A = 7.39 × 10^{-12} m/s.Pa B = 20.55 × 10^{-8} m/s R (NaCl) = 89.99% S = 400 µm	[26]
2g PSF 2% MPD/0.1% TMC 0.25% ZnO@PMMA in aqueous solution	DI water	1M NaCl	ambient	0.1 L/min	14.6	2.2	—	—	A = 2.32 LMH/bar B = 0.28 LMH R (NaCl) = 97.7% S = 693 µm	[27]

Support Layer Polyamide Active Layer Nanomaterial	Experimental Operating Conditions				FO Performance				Intrinsic Properties	Reference
					FS–AL (FO Mode)		DS–AL (PRO Mode)			
	Feed Solution	Draw Solution	Temp.	Flow Rate	Jw; LMH	Js; gMH	Jw; LMH	Js; gMH		
16% PSF/6% PVP/2% LiCl 2% MPD/0.1% TMC 0.5% Al_2O_3 in dope solution 0.05% Al_2O_3 in organic solution	DI water	1M NaCl	—	18.5 cm/s	27.6	7.1	—	—	A = 8.43 LMH/bar B = 1.66 LMH	[28]
14% PES/2% PVP 2% MPD/0.1% TMC 0.2% Fe_3O_4 in dope solution	10 mM NaCl	2M NaCl	room	0.8 L/min	28.8	14.7	38.08	20.1	A = 8.55 × 10^{-12} m/s.Pa B = 15.6 × 10^{-8} m/s R (NaCl) = 93.2% S = 420 μm	[29]
17.41% PSF/0.5% PVP/0.5% nano-filler 2% MPD/0.1% TMC 0.5% TiO_2 and 0.5% GO in dope solution	DI water	2M NaCl	—	2.5 cm/s	23.5	2.7	30.5	4.4	A = 1.61 × 10^{-12} m/s.Pa B = 1.44 × 10^{-8} m/s R (NaCl) = 91.1% S = 200 μm	[30]
18% PES/2% PEG-200 2% MPD/0.1% TMC 0.2% ZnO/SiO_2 in dope solution	DI water	1M NaCl	25 °C	8.3 cm/s	33.5	12.23	50.1	18.22	A = 3.47 LMH/bar B = 4.01 LMH R (NaCl) = 78.6% S = 297 μm	[31]
18% PVDF/3% PVP 2% MPD/0.1% TMC 0.75% SiO_2@MWCNT in dope solution	DI water	1M NaCl	—	0.3 L/min	22.1	4.1	28.6	8.05	A = 1.21 LMH/bar B = 0.12 LMH R (NaCl) = 93.6% S = 240.5 μm	[32]
14% PES/2% PVP 2% MPD/0.1% TMC 0.2% Fe_3O_4/ZnO in aqueous solution	10 mM NaCl	2M NaCl	23 °C	0.8 L/min	29.3	5.6	—	—	A = 8.24 × 10^{-12} m/s.Pa B = 7.88 × 10^{-8} m/sR (NaCl) = 98.5%S = 400 μm	[33]

2.1. GO Nanoparticle

Graphene oxide (GO) is a carbon-based nanomaterial that has a single layer with a carbonous structure that is sp2-bonded. Interestingly, GO nanosheets showed a marked potential as a platform material for novel nanocomposite membrane design due to its high surface area and stronger chemical stability as well as higher hydrophilicity and excellent anti-fouling characteristics [10]. Moreover, GO has contain many functional groups such as hydroxyl (O–H), carboxyl (C–OOH), carbonyl (C=O), and epoxy (C–C) groups because of its nature of hydrophilicity [34]. Due to its many benefits, GO is compatible with many polymers and can be incorporated into polymeric membranes [35]. In the year 2015, Park et al. [12] created a PSF/GO support layer for TFC-FO membranes by integrating GO nanosheets (zero to 1.0 wt.%) into PSF substrates. It was demonstrated that GO-containing TFC membranes increased hydrophilicity and a lower structural parameter of the membrane. Upon optimal addition of 0.25 wt.% GO, the structural properties of the support layer improved, and also the formation of an effective polyamide layer. As a result, GO modified membrane exhibit higher water flux (19.77 LMH) and salt rejection (98.71%) compared with an unmodified membrane (6.08 LMH, 97.04%). However, GO loading above 0.5 wt.% caused a lower water flux due to weak GO dispersion in PSF, which resulted in the creation of a membrane with sponge-like support structures that had lower porosity and smaller pore size. In addition to the ineffective creation of a selective polyamide layer that harms the salt rejection of TFC-FO membranes. Along the same

lines, Idris et al. [13] incorporated GO (in range as 0 to 1.0 wt.%) in the casting solution of a TFC FO membrane to improve osmotic power generation. At the optimal addition of 0.25 wt.% GO, the incorporation of GO not only promoted a power density of 8.36 W/m^2 but is also able to withstand an applied pressure over 15 bar. On the other hand, the effect of different-sized GO flakes ranging from 0.01 to 1.06 μm^2 was studied by Akther et al. [14] on the morphology and performance of the polyamide layer. They observed that the small GO flakes (MGO-8, tip sonicated for 8 h) resulted in a more uniform GO dispersion which reduced the defects of the PA layer; thus, membrane flux and selectivity improved. Whereas, the large GO flakes deteriorated the membrane performance by creating impervious regions that impeded the interaction between monomers during the interfacial polymerization process resulting in defective PA layer formation. Moreover, Saeedi-Jurkuyeh et al. [15] added GO in a selective layer and they found that these membranes can be utilized to remove heavy metals from synthetic and industrial wastewater. Pb, Cd, and Cr had the highest rejection rates of 99.9%, 99.7%, and 98.3%, respectively. Latest developments, Li et al. [36] fabricated a TFC-FO membrane for improving the water flux and anti-biofouling ability in which the substrate (TFN-S), polyamide layer (TFN-A), or both (TFN-S+A) were modified by GO. They discovered that TFN-S could greatly improve the water flux because improve the porous structure and porosity, whereas TFN-A and TFN-S+A membrane exhibited higher salt rejection and biofouling mitigation because of lower roughness and greater hydrophilicity.

2.2. Zeolite Nanoparticle

Zeolite is a microporous, crystalline aluminosilicate with a 3D tetrahedral framework structure and its unique features make it a material with great selectivity, high specific capacity, and exceptional resistance to chemical, biological, mechanical, or thermal stress [37]. In the year 2012, Ma et al. [16] studied incorporating zeolite NaY nanoparticles into a polyamide selective layer to enhance the performance of TFN-FO membranes. They dispersed nanoparticles in the organic solution (0.05 wt.% TMC). The addition of zeolite nanoparticles in the range of 0–0.2 wt.% changed the surface morphology, roughness, and contact angle, all of which influenced the separation properties and performance of the fabricated membranes. This addition also resulted in enhanced water flux and salt rejection at a relatively low zeolite loading level. However, a high (0.4 wt.%) zeolite loading may aid in the formation of a relatively thicker polyamide layer, which reduces water permeability and enhances salt rejection. Contrarily, the feasibility of incorporating zeolite NaY nanoparticles into a PSF-based substrate has been studied by Ma et al. [17] to improve the permeability of the polyamide layer. They found that features from zeolite loading (0.5 wt.%) improved surface porosity from 81.4% to 79.8%, reduced the contact angle from 53° to 50°, and provided additional water pathways as well as thin, sponge-like skin and a highly permeable sub-layer with straight, needle-like pores. These pores ensured a low S value and thus reducing the effect of ICP. Meanwhile, the overall thickness and contact angle of the substrate were slightly reduced with increasing zeolite loading (1 wt.%). Moreover, surface defects and unevenness with overloaded may adversely affect the integrity of the polyamide layer formed on it. Similarly, nanostructured zeolites (i.e., clinoptilolite) at a concentration of 0–0.6 wt.% were inserted into the matrix of a PES substrate and shown to be efficient in minimizing ICP effects [18].

2.3. TiO$_2$ Nanoparticle

Titanium dioxide (TiO$_2$) is an inorganic nanoparticle and is widely used to improve membrane hydrophilic performance since its commercially available, inexpensive, has photocatalytic behaviour, is chemically stable, has zero toxicity, and is anti-fouling [38][39]. Moreover, the TiO$_2$ surface features a thin layer of water molecules, which gives it a high degree of hydrophilicity. Moreover, the photocatalytic nature of TiO$_2$ aid to improve its self-cleaning ability to keep its surface clean [40]. The improved water flux can be attributed to the incorporation of modified TiO$_2$ nanoparticles, in the range of 0 to 0.1 wt.%, into the polyamide layer, which may be due to decreased roughness (112.48–72 nm), and increased porosity (77–81%) as well as the reduced contact angle (66.5–50.5°). Further increase in TiO$_2$ concentration led to reduced solute flux. Moreover, the modification of nanoparticles increased the hydrophilic amide bonds (–NH$_2$) on the surface of the membrane. Thus, the incorporation of TiO$_2$ nanoparticles on the active layer allows water droplets to easily expand on it.

2.4. SiO$_2$ Nanoparticle

Silicon oxide (SiO$_2$) nanoparticles are one of the most inspirational types of inorganic nanomaterials due to their unique properties such as strong surface energy, little size, thermal resistance, nontoxic, inert nature, and fine hang in polymer solution or aqueous solution. It is also inexpensive and widely available [22][41]. In the year 2014, Niksefat et al. [23] reported on SiO$_2$ incorporated into the active layer of the membrane via interfacial polymerization of MPD and TMC to enhance the membrane parameters. PSF was used for making the base layer, and SiO$_2$ (i.e., in a range of 0.01–0.1 wt.%) was added to the aqueous phase (2 wt.% MPD). This study demonstrated that the improvement in water flux was caused by a decreased structural parameter (435–376 μm) which contributes to a low CP effect and thus a reduction in flux resistance, and improved membrane surface roughness (30.3–134.2 nm) and hydrophilicity (82–44°) which may be

caused by the accumulation of SiO_2 on the membrane surface. TFN membrane with 0.05 wt.% SiO_2 provided the best water flux and salt rejection. Moreover, the overloading of silica (0.1 wt.%) may not be beneficial to FO performance and may potentially harm membrane properties. Another study has also proved that the insertion of SiO_2 nanoparticles into the membrane support layer improved the hydrophilicity and porosity of the membrane which can effectively reduce the ICP effect. Moreover, water permeability and salt rejection were found to have improved upon the addition of SiO_2 up to 5 wt%, but it could not enhance the FO membrane's selectivity. It is worth mentioning that overloading of SiO_2 content (3 and 5 wt.%) may shrink pores on the membrane surface and this did not result in serious defects on the polyamide layer. However, the water flux was found to have increased from 9.1 to 22.3 LMH and 18.2 to 41.9 LMH in AL-FS and AL-DS orientation, respectively [24]. Most recently, Islam et al. [25] incorporated super-hydrophilic SiO_2 in both the electro-spun nylon-6 (N6) substrate and the polyamide active layer to fabricate the TFN membrane. The prepared membrane exhibited high water flux and antifouling due to 24.1 MPa tensile strength with a 14° water contact angle. In addition, the flux recoveries after fouling and cleaning operations were 98% and 95.15% for sodium alginate (SA) foulant and calcium sulfate ($CaSO_4$) scalant, respectively. The developed TFN membrane's structural stability was also enhanced by a strong contact between the selective layer and the substrate.

2.5. ZnO Nanoparticle

Zinc oxide (ZnO) has drawn increased attention since it is environmentally friendly, mechanically and chemically stable, non-toxic, and low-cost [26][42]. In addition, it is one of the best materials for creating composite membranes due to its higher surface area, increased hydrophilicity, and higher fouling resistance [43]. In the year 2018, Mansouri et al. [26] studied the influence of hydrophilic and hydrophobic modified ZnO nanoparticles incorporated in the PES matrix on FO membrane properties. Adding 0.5 wt% ZnO, the contact angle of the hydrophilic PES sublayer decreased from 56.04° to 31.57°, while it increased for the hydrophobic PES sublayer to 78.4°. Additionally, loading hydrophilic ZnO nanoparticles enhanced the pore size and porosity of the PES sublayer, while loading hydrophobic ZnO nanoparticles lowered them. Moreover, they noted that the modified PES sublayer with higher surface hydrophilicity absorbed more MPD; thus, more MPD molecules were available in the porous media to diffuse into the organic phase, resulting in a thinner PA layer with a higher degree of cross-linking due to interaction between MPD and the sublayer compared to those of hydrophobic membrane. Moreover, the TFC membranes fabricated over hydrophilic substrates revealed higher water permeability (2.66 LMH/bar) and NaCl rejection (92.12%) than those fabricated over hydrophobic substrates (1.4 LMH/bar, 89.99%). In another research study, Ghalavand et al. [27] used a poly (methyl methacrylate) (PMMA) grafted ZnO nanoparticle, in a range of 0–0.5%, to build a novel nanofiller within the PSF support layer which was coated with in situ polymerized polyamide. By the addition of ZnO@PMMA nanoparticles to the support layer forming a nano-composite sublayer, its hydrophilicity increased for the TFN membranes.

2.6. Other Nanoparticles

Ding et al. [28] employed hydrophilic aluminum oxide (Al_2O_3) nanoparticles as additives in both PSF support and polyamide layers to additionally create water channels in the substrate leading to increment in mass transfer and water permeability because they possess several advantages such as a high surface area, a large pore volume, and a high porosity. It was found that the addition of 0.5 wt.% Al_2O_3 NPs improved the substrate morphology, which involved high porosity (71.1%) and pore size (34.1 nm), hydrophilicity (67.7°), roughness (25.35 nm), and a finger-like structure was formed. Moreover, the structural parameter was decreased significantly from 1422 μm (pure PS substrate) to 1028 μm, which lead to lower ICP impacts. Moreover, the addition of 0.05 wt.% Al_2O_3 NPs to PA layer lead to higher roughness and thickness of the selective layer due to the formation of large "leaf-like" morphological structures and NPs aggregation. It was anticipated that the higher roughness, hydrophilicity, and large surface area of the active layer would result in high water flux and reduced salt diffusion. They also monitored that the modified TFN membrane demonstrated excellent FO performance and stability over long-term operation. In another study by Darabi et al. [29], ferrous ferric oxide (Fe_3O_4) nanoparticles were incorporated as inorganic nanofiller ranging from zero to 0.5 wt% into a PES substrate matrix because of its multiple benefits, including low toxicity, good biocompatibility, high surface area, chemical stability, and unique magnetic characteristics. The addition of 0.2 wt.% Fe_3O_4 to the substrate improves its main characteristics in terms of hydrophilicity (62°), porosity (87%), pore size (36.5 nm), cross-sectional morphology (longer finger-like structure), roughness (41.48 nm), and strength (3.12 MPa). This structure is preferred for FO membranes because it results in less resistance to the diffusion of water and salt and thus reduces unwanted the ICP effect of membranes. While Zirehpour et al. [11] established nano-sized metal–organic framework (MOF) particles from silver (I) and 1,3,5-benzene tricarboxylic acid. 0.04 wt.% MOF as a new category of organic/inorganic hybrid materials consisting of metal ions or clusters coordinated to organic ligands was added into the polyamide layer of membranes to improve the structure of TFC membranes for seawater desalination. This nanoparticle improved the active layer's hydrophilicity and transport characteristics while not affecting selectivity due to the good affinity between the MOF and the PA layer. They also

reported that the TFN membrane exhibited 129% higher pure water permeability in comparison with the TFC membrane as well as significantly improved performance stability throughout the testing interval.

2.7. Mixture Nanoparticles

In past years, research efforts contributed to the preparation of membranes modified with a mixture of nanoparticles. Sirinupong et al. [30] incorporated titanium dioxide/graphene oxide (TiO_2/GO) as a nanofiller into a PSF-based substrate to improve the TFC membrane performance during FO applications. Rastgar et al. [31] prepared TFN-PA membranes by introducing the ZnO-SiO$_2$ core–shell nanoparticles (ZSCSNPs) into the PSF substrate as a good candidate for improving FO membrane performance. ZSCSNPs, which were more hydrophilic than ZNP, were created by first preparing ZNP using the sol-gel process and then coating them with hydrophilic SiO_2. They found that both ZNP and ZSCSNP had the same effect but the effect of ZSCSNP was stronger. In RO tests, the NaCl rejection was almost the same after the addition of either of the two NPs due to the negligible difference in the size of the utilized NPs, i.e., 30 and 50 nm. Whereas in FO tests, the water flux of ZSCSNPs TFN membrane was higher due to the higher hydrophilicity and lower roughness of ZSCSNP than that of ZNP. Zhang et al. [32] incorporated SiO_2/MWNTs obtained from the hydrolysis of tetraethyl orthosilicate (TEOS) on aminated multiwall carbon nanotubes (MWCNT) in a PVDF substrate to fabricate a TFN-FO membrane. Optimal membrane morphology with an appropriate pore size distribution, increase in porosity and roughness, and decrease in contact angle are all the epitome of the addition of SiO_2@MWNTs hybrid nanomaterial. These changes finally facilitated the production of a defect-free polyamide layer. Water movement was aided by the extra mass transfer channels created by the SiO2@MWNTs in the substrate when the SiO_2@MWNTs fraction was 0.75 wt.%. Darabi et al. [33] incorporated magnetite/zinc oxide (Fe_3O_4/ZnO) into both the upper and sub-layer of an FO membrane to improve its properties and performance. The inclusion of Fe_3O_4/ZnO resulted in a finger-like structure in the substrate and a leaf-like surface in the PA layer. Furthermore, photocatalytic Fe_3O_4/ZnO nanocomposite activation increased the hydrophilicity of TFN membranes under UV irradiation. Due to these morphological changes, the TFN membrane achieves a higher water flux of 78% than the TFC membrane, which also achieves the highest NaCl rejection (96.5%), and the lowest S (0.4 mm) compared to the TFC membrane (96.3%, 0.78 mm). Rastgar et al. [44] observed a 117.4% increase in FO water flux compared to the TFC membrane due to the enhanced wettability, smoother surface, and porous structure of the polyamide layer by introducing a new approach for magnetically modifying GO within the polyamide layer to create TFN-MMGO/Fe_3O_4 membranes. Moreover, these morphological modifications lead to reducing fouling tendency: (I) hydrophilicity, which prevents hydrophobic foulants from adhering to the membrane surface by forming a thick layer of water molecules through hydrogen bonding; (II) smoother, which reduces the area available for membrane-foulant interactions; and (III) the presence of negative carboxyl groups on the surface.

References

1. Wang, Z.; Liu, K.; Gao, Y.; Li, G.; Li, Z.; Wang, Q.; Guo, L.; Liu, T.; Al-Namazi, M.A.; Li, S. Removal and Fouling Influence of Microplastics in Fertilizer Driven Forward Osmosis for Wastewater Reclamation. Membranes 2021, 11, 845.

2. Mendoza, E.; Buttiglieri, G.; Blandin, G.; Comas, J. Exploring the limitations of forward osmosis for direct hydroponic fertigation: Impact of ion transfer and fertilizer composition on effective dilution. J. Environ. Manag. 2022, 305, 114339.

3. Abbas, T.K.; Rashid, K.T.; Alsalhy, Q.F. NaY zeolite-polyethersulfone-modified membranes for the removal of cesium-137 from liquid radioactive waste. Chem. Eng. Res. Des. 2022, 179, 535–548.

4. Rashid, W.T.; Alkadir, I.A.; Jalhoom, M.G.; Rashid, K.T. (Polyphenyl Sulfone-Polyether Sulfone) Blending to Performance Flat Sheet Membrane to Remove Some Heavy and Radioactive Elements from Phosphogypsum. Waste Eng. Technol. J. 2021, 39, 382–393.

5. Al-Bahate, M.J.; Shabeeb, K.M.; Khalil, B.I. Effect of Polyvinyl Pyrrolidone on Polyvinyl Chloride-Graft-Acrylamide Membranes. Eng. Technol. J. 2020, 38, 1205–1315.

6. Al-Shaeli, M.; Al-Juboori, R.A.; Al Aani, S.; Ladewig, B.P.; Hilal, N. Natural and recycled materials for sustainable membrane modification: Recent trends and prospects. Sci. Total Environ. 2022, 838, 156014.

7. Klaysom, C.; Cath, T.Y.; Depuydt, T.; Vankelecom, I.F. Forward and pressure retarded osmosis: Potential solutions for global challenges in energy and water supply. Chem. Soc. Rev. 2013, 42, 6959–6989.

8. Long, Q.; Wang, Y. Novel carboxyethyl amine sodium salts as draw solutes with superior forward osmosis performance. AIChE J. 2016, 62, 1226–1235.

9. Mohammadifakhr, M.; de Grooth, J.; Roesink, H.D.W.; Kemperman, A.J.B. Forward Osmosis: A Critical Review. Processes 2020, 8, 404.

10. Yadav, S.; Saleem, H.; Ibrar, I.; Naji, O.; Hawari, A.A.; Alanezi, A.A.; Zaidi, S.J.; Altaee, A.; Zhou, J. Recent developments in forward osmosis membranes using carbon-based nanomaterials. Desalination 2020, 482, 114375.

11. Zirehpour, A.; Rahimpour, A.; Ulbricht, M. Nano-sized metal organic framework to improve the structural properties and desalination performance of thin film composite forward osmosis membrane. J. Membr. Sci. 2017, 531, 59–67.

12. Park, M.J.; Phuntsho, S.; He, T.; Nisola, G.M.; Tijing, L.D.; Li, X.-M.; Chen, G.; Chung, W.-J.; Shon, H.K. Graphene oxide incorporated polysulfone substrate for the fabrication of flat-sheet thin-film composite forward osmosis membranes. J. Membr. Sci. 2015, 493, 496–507.

13. Idris, S.N.; Jullok, N.; Lau, W.J.; Ong, H.L.; Dong, C.-D. Graphene oxide incorporated polysulfone substrate for flat sheet thin film nanocomposite pressure retarded osmosis membrane. Membranes 2020, 10, 416.

14. Akther, N.; Yuan, Z.; Chen, Y.; Lim, S.; Phuntsho, S.; Ghaffour, N.; Matsuyama, H.; Shon, H. Influence of graphene oxide lateral size on the properties and performances of forward osmosis membrane. Desalination 2020, 484, 114421.

15. Saeedi-Jurkuyeh, A.; Jafari, A.J.; Kalantary, R.R.; Esrafili, A. A novel synthetic thin-film nanocomposite forward osmosis membrane modified by graphene oxide and polyethylene glycol for heavy metals removal from aqueous solutions. React. Funct. Polym. 2020, 146, 104397.

16. Ma, N.; Wei, J.; Liao, R.; Tang, C.Y. Zeolite-polyamide thin film nanocomposite membranes: Towards enhanced performance for forward osmosis. J. Membr. Sci. 2012, 405, 149–157.

17. Ma, N.; Wei, J.; Qi, S.; Zhao, Y.; Gao, Y.; Tang, C.Y. Nanocomposite substrates for controlling internal concentration polarization in forward osmosis membranes. J. Membr. Sci. 2013, 441, 54–62.

18. Salehi, T.M.; Peyravi, M.; Jahanshahi, M.; Lau, W.-J.; Rad, A.S. Impacts of zeolite nanoparticles on substrate properties of thin film nanocomposite membranes for engineered osmosis. J. Nanoparticle Res. 2018, 20, 1–15.

19. Emadzadeh, D.; Lau, W.J.; Matsuura, T.; Ismail, A.F.; Rahbari-Sisakht, M. Synthesis and characterization of thin film nanocomposite forward osmosis membrane with hydrophilic nanocomposite support to reduce internal concentration polarization. J. Membr. Sci. 2014, 449, 74–85.

20. Emadzadeh, D.; Lau, W.J.; Matsuura, T.; Rahbari-Sisakht, M.; Ismail, A.F. A novel thin film composite forward osmosis membrane prepared from PSf–TiO2 nanocomposite substrate for water desalination. Chem. Eng. J. 2014, 237, 70–80.

21. Amini, M.; Rahimpour, A.; Jahanshahi, M. Forward osmosis application of modified TiO2-polyamide thin film nanocomposite membranes. Desalinat. Water Treat. 2016, 57, 14013–14023.

22. Tharayil, J.; Manaf, A. Effect of different inorganic draw solutes on SiNPs-TFN membrane for forward osmosis desalination. Int. J. Environ. Sci. Technol. 2022, 19, 289–298.

23. Niksefat, N.; Jahanshahi, M.; Rahimpour, A. The effect of SiO2 nanoparticles on morphology and performance of thin film composite membranes for forward osmosis application. Desalination 2014, 343, 140–146.

24. Huang, Y.; Jin, H.; Yu, P.; Luo, Y. Polyamide thin-film composite membrane based on nano-silica modified polysulfone microporous support layer for forward osmosis. Desalinat. Water Treat. 2016, 57, 20177–20187.

25. Islam, M.S.; Touati, K.; Rahaman, M.S. High flux and antifouling thin-film nanocomposite forward osmosis membrane with ingrained silica nanoparticles. ACS EST Eng. 2021, 1, 467–477.

26. Mansouri, S.; Khalili, S.; Peyravi, M.; Jahanshahi, M.; Darabi, R.R.; Ardeshiri, F.; Rad, A.S. Sublayer assisted by hydrophilic and hydrophobic ZnO nanoparticles toward engineered osmosis process. Korean J. Chem. Eng. 2018, 35, 2256–2268.

27. Ghalavand, R.; Mokhtary, M.; Shakeri, A.; Alizadeh, O. incorporated PSf substrate for improving thin-film composite membrane performance in forward osmosis process. Chem. Eng. Res. Des. 2022, 177, 594–603.

28. Ding, W.; Li, Y.; Bao, M.; Zhang, J.; Zhang, C.; Lu, J. Highly permeable and stable forward osmosis (FO) membrane based on the incorporation of Al2O3 nanoparticles into both substrate and polyamide active layer. RSC Adv. 2017, 7, 40311–40320.

29. Darabi, R.R.; Peyravi, M.; Jahanshahi, M.; Amiri, A.A.Q. Decreasing ICP of forward osmosis (TFN-FO) membrane through modifying PES-Fe3O4 nanocomposite substrate. Korean J. Chem. Eng. 2017, 34, 2311–2324.

30. Sirinupong, T.; Youravong, W.; Tirawat, D.; Lau, W.; Lai, G.; Ismail, A. Synthesis and characterization of thin film composite membranes made of PSF-TiO2/GO nanocomposite substrate for forward osmosis applications. Arab. J. Chem. 2018, 11, 1144–1153.

31. Rastgar, M.; Shakeri, A.; Bozorg, A.; Salehi, H.; Saadattalab, V. Impact of nanoparticles surface characteristics on pore structure and performance of forward osmosis membranes. Desalination 2017, 421, 179–189.

32. Zhang, X.; Shen, L.; Guan, C.-Y.; Liu, C.-X.; Lang, W.-Z.; Wang, Y. Construction of MWNTs incorporated PVDF substrate for reducing internal concentration polarization in forward osmosis. J. Membr. Sci. 2018, 564, 328–341.

33. Darabi, R.R.; Jahanshahi, M.; Peyravi, M. A support assisted by photocatalytic Fe3O4/ZnO nanocomposite for thin-film forward osmosis membrane. Chem. Eng. Res. Des. 2018, 133, 11–25.

34. Sadiq, A.J.; Awad, E.S.; Shabeeb, K.M.; Khalil, B.I.; Al-Jubouri, S.M.; Sabirova, T.; Tretyakova, N.; Majdi, H.S.; Alsalhy, Q.F.; Braihi, A.J. Comparative study of embedded functionalised MWCNTs and GO in Ultrafiltration (UF) PVC membrane: Interaction mechanisms and performance. Int. J. Environ. Anal. Chem. 2020, 103, 415–436.

35. Al-Maliki, R.M.; Alsalhy, Q.F.; Al-Jubouri, S.; Salih, I.K.; AbdulRazak, A.A.; Shehab, M.A.; Németh, Z.; Hernadi, K. Classification of Nanomaterials and the Effect of Graphene Oxide (GO) and Recently Developed Nanoparticles on the Ultrafiltration Membrane and Their Applications: A Review. Membranes 2022, 12, 1043.

36. Li, Y.; Yang, Y.; Li, C.; Hou, L.-a. Comparison of performance and biofouling resistance of thin-film composite forward osmosis membranes with substrate/active layer modified by graphene oxide. RSC Adv. 2019, 9, 6502–6509.

37. Perego, C.; Bagatin, R.; Tagliabue, M.; Vignola, R. Zeolites and related mesoporous materials for multi-talented environmental solutions. Microporous Mesoporous Mater. 2013, 166, 37–49.

38. Zhang, X.; Xiong, S.; Liu, C.-X.; Shen, L.; Ding, C.; Guan, C.-Y.; Wang, Y. Confining migration of amine monomer during interfacial polymerization for constructing thin-film composite forward osmosis membrane with low fouling propensity. Chem. Eng. Sci. 2019, 207, 54–68.

39. Ghanbari, M.; Emadzadeh, D.; Lau, W.J.; Matsuura, T.; Davoody, M.; Ismail, A.F. Super hydrophilic TiO2/HNT nanocomposites as a new approach for fabrication of high performance thin film nanocomposite membranes for FO application. Desalination 2015, 371, 104–114.

40. Al-Jadir, T.; Alardhi, S.M.; Alheety, M.A.; Najim, A.A.; Salih, I.K.; Al-Furaiji, M.; Alsalhy, Q.F. Fabrication and characterization of polyphenylsulfone/titanium oxide nanocomposite membranes for oily wastewater treatment. J. Ecol. Eng. 2022, 23, 1–13.

41. Al-Araji, D.D.; Al-Ani, F.H.; Alsalhy, Q.F. Modification of polyethersulfone membranes by Polyethyleneimine (PEI) grafted Silica nanoparticles and their application for textile wastewater treatment. Environ. Technol. 2022, 1–17.

42. Alsalhy, Q.F.; Al-Ani, F.H.; Al-Najar, A.E.; Jabuk, S.I.A. A study of the effect of embedding ZnO-NPs on PVC membrane performance use in actual hospital wastewater treatment by membrane bioreactor. Chem. Eng. Process.-Process Intensif. 2018, 130, 262–274.

43. Amini, M.; Seifi, M.; Akbari, A.; Hosseinifard, M. Polyamide-zinc oxide-based thin film nanocomposite membranes: Towards improved performance for forward osmosis. Polyhedron 2020, 179, 114362.

44. Rastgar, M.; Shakeri, A.; Bozorg, A.; Salehi, H.; Saadattalab, V. Highly-efficient forward osmosis membrane tailored by magnetically responsive graphene oxide/Fe3O4 nanohybrid. Appl. Surf. Sci. 2018, 441, 923–935.